Expansion of the sagittal suture induces proliferation of skeletal stem cells and sustains endogenous calvarial bone regeneration

Zahra A. Aldawood[a,b,1] (ID), Luigi Mancinelli[c,d,1] (ID), Xuehui Geng[c,d], Shu-Chi A. Yeh[e] (ID), Roberta Di Carlo[c,d], Taiana C. Leite[c,d], Jonas Gustafson[f] (ID), Katarzyna Wilk[a], Joseph Yozgatian[a], Sasan Garakani[a], Seyed Hossein Bassir[a], Michael L. Cunningham[f,g] (ID), Charles P. Lin[e], and Giuseppe Intini[c,d,h,i,j,2] (ID)

In newborn humans, and up to approximately 2 y of age, calvarial bone defects can naturally regenerate. This remarkable regeneration potential is also found in newborn mice and is absent in adult mice. Since previous studies showed that the mouse calvarial sutures are reservoirs of calvarial skeletal stem cells (cSSCs), which are the cells responsible for calvarial bone regeneration, here we hypothesized that the regenerative potential of the newborn mouse calvaria is due to a significant amount of cSSCs present in the newborn expanding sutures. Thus, we tested whether such regenerative potential can be reverse engineered in adult mice by artificially inducing an increase of the cSSCs resident within the adult calvarial sutures. First, we analyzed the cellular composition of the calvarial sutures in newborn and in older mice, up to 14-mo-old mice, showing that the sutures of the younger mice are enriched in cSSCs. Then, we demonstrated that a controlled mechanical expansion of the functionally closed sagittal sutures of adult mice induces a significant increase of the cSSCs. Finally, we showed that if a calvarial critical size bone defect is created simultaneously to the mechanical expansion of the sagittal suture, it fully regenerates without the need for additional therapeutic aids. Using a genetic blockade system, we further demonstrate that this endogenous regeneration is mediated by the canonical Wnt signaling. This study shows that controlled mechanical forces can harness the cSSCs and induce calvarial bone regeneration. Similar harnessing strategies may be used to develop novel and more effective bone regeneration autotherapies.

calvarial skeletal stem cells | calvarial sutures | *Prx1* | *Prrx1* | SSC

Despite recent advancements, bone regeneration of craniofacial defects due to trauma, congenital abnormalities, or cancer remains a difficult task and represents a serious health burden (1–3). Available therapeutic aids, including those based on implantable biomaterials and recombinant growth factors, present limitations in terms of efficacy and safety (4–7). New approaches utilizing stem cells have also been tested with limited success (8, 9).

In what appears to be a paradigm shift in craniofacial biology (10), we and others have determined that the postnatal mouse calvarial sutures, in addition to acting as compliant connectors between calvarial bones (synarthroses), serve as reservoirs for calvarial skeletal stem cells (cSSCs) that contribute to calvarial bone regeneration (11–14). For instance, in our studies we showed that cSSCs expressing *Prx1/Prrx1*, a transcription factor expressed in the mesenchyme during craniofacial and limb development (11, 12), are required for regeneration of calvarial bone defects, and that their progeny is responsible for the bone regeneration process (13). Importantly, our previous studies also showed that the number of *Prx1/Prrx1* expressing cells declines with aging, while the total number of the cells resident within the sutures remains stable after the sutures are fully developed (13).

Other investigators identified cells expressing *Gli1* [Zhao et al. (14)] or *Axin2* [Maruyama et al. (15)] as cells of the calvarial sutures with stem cell qualities similar to those of the *Prx1/Prrx1* expressing cells. More recently, Debnath et al. (16) also proposed expression of *Cathepsin K* (*Ctsk*) as another marker of the cSSCs. The identification of the cSSCs and the characterization of their roles in calvarial bone regeneration warrant additional studies aimed at understanding whether cSSCs can be harnessed for more effective craniofacial bone regenerative therapies.

Of much interest to bone regenerative studies, it has been described that in children up to 2 y of age, regeneration of calvarial defects can occur naturally and without therapeutic aids (i.e., implantation of biomaterials of osteogenic tissues) (17, 18). This exceptional regenerative potential coincides with the existence of calvarial sutures in rapid expansion and is lost around 2 y of age, when a substantial functional closure of the sutures occurs (19, 20). Importantly, a similar age-related regenerative potential is also observed in mice, whose calvarial bone and suture development is analogous to humans. In fact, mice are utilized to study craniofacial development, craniofacial pathologies (i.e., craniosynostosis), and to

Significance

This work describes the discovery that an "activation" of a calvarial suture, in the form of a controlled mechanical expansion, can increase the number of calvarial skeletal stem cells (cSSCs) present in the suture and can, consequently, sustain the regeneration of calvarial bone defects that are otherwise unable to heal. Significantly, we show that using this strategy, bone regeneration occurs without implantations of biomaterials or other osteogenic tissues within the bone defects. Thus, mechanically induced suture expansion could be utilized to harness cSSCs in challenging calvarial bone regeneration procedures. The same strategy could be validated to activate other skeletal stem cell niches of the skeleton and foster regeneration of bone defects of other skeletal segments.

develop new bone regeneration approaches (20–25). Therefore, here we posited that the calvarial bone regeneration potential observed in infant humans and mice is due to a significant number of cSSCs present within the expanding sutures. This hypothesis is supported by evidence showing that, at least in mice, the number of cSSCs declines with aging (13) and that a certain critical amount of cSSCs is required for the calvarial regeneration process to occur (13, 26). In fact, as shown in our previous studies, a reduction of 80% of the *Prx1/Prrx1* expressing cells, induced by means of expression of the Diphtheria toxin gene, significantly impairs regeneration of otherwise spontaneously healing calvarial bone defects (13). Moreover, the distance of a calvarial bone defect from the suture greatly influences the regenerating amount of bone, indicating that bone regeneration can only occur if a sufficient number of cSSCs, or a sufficient number of their progeny, can reach the bone defect (26). Therefore, in the present work we tested our hypothesis by artificially inducing an increase of cSSCs within the functionally closed calvarial sutures of skeletally mature 2-mo-old (8 wk old) mice and by testing the effect of the increase on the regeneration of calvarial bone defects otherwise unable to spontaneously regenerate (calvarial critical size defect, hereafter identified as c-CSD).

First, we employed single cell RNA sequencing (scRNA-seq) to compare the cellular composition of the calvarial sutures in mice of different ages, from the rapidly expanding calvarial sutures of 4-d-old mice to the fully developed and aged sutures of 14-mo-old mice. Such evaluation confirmed that a significantly higher number of cSSCs are present in the developing open sutures of the 4-d-old mice. Then, utilizing scRNA-seq and intravital microscopy (IVM) (13, 27, 28), we demonstrated that the mechanical expansion of the sagittal suture of a skeletally mature 2-mo-old mouse is able to induce proliferation of the sagittal suture cSSCs. Finally, by means of microcomputed tomography (μCT) and histological evaluations we showed that the mechanical expansion sustains full regeneration of a c-CSD created in the parietal bone, and by means of mouse genetics approaches we showed that the regeneration process is mediated by Wnt signaling. Importantly, by further showing that *Prx1/Prrx1* expressing cells are present in human calvarial sutures, our studies indicate that the shown mouse findings could potentially be translated to humans.

Results

Single cell RNA-seq Profiling Identifies a Significantly High Number of cSSCs in the Calvarial Sutures of 4-d-old Mice Versus Older Mice.
To evaluate and identify different populations of cells in the calvarial sutures of young and older mice, we performed scRNA-seq analyses. We utilized sutures explanted from 4-d-old mice, an age when the suture is actively and naturally expanding, and sutures explanted from skeletally mature 2-mo-old, 4-mo-old, and 14-mo-old mice, representing ages when the sutures are functionally closed and have matured into synarthroses (29). In sutures of 4-d-old mice, an unbiased cluster analysis of all the isolated cells identified various cell clusters, which include cell types of the hematopoietic lineage, epithelial lineage, and osteogenic lineage (Fig. 1*A*) (refer to *Materials and Methods* for the methodology utilized for the classification of the clusters). Three clusters, named osteogenic cells cluster 1, 2, and 3, make up all the cells of osteogenic lineage. The analysis of the calvarial sutures of 2-mo-old, 4-mo-old, and of 14-mo-old mice also reveals the presence of cells of the hematopoietic lineage and of the osteogenic lineage (Fig. 1 *B–D*). However, at these ages, only one cluster containing a small number of cells could be identified as constituent of the osteogenic lineage. A quantification of the total osteogenic cells across all ages (indicated as percentage of

the total cells evaluated, representing a more accurate quantitative parameter since the final number of cells used in each scRNA-seq assay variates from experiment to experiment) confirms that in the sutures of 4-d-old mice, the osteogenic cells are ~44% of all the cells, whereas in 2-mo-old mice they decrease to ~5% and in 4 mo old and 14 mo old they become less than 0.3% of all cells (Fig. 1*E*). Conversely, non-osteogenic cells increase with aging, spanning from ~56% in 4-d-old mice to ~95% in 2-mo-old mice, up to more than 99% in 4-mo and 14-mo-old mice (Fig. 1*E*).

We then interrogated the scRNA-seq data to distinguish and quantify, across the four different ages, cells expressing *Prx1/Prrx1*, *Ctsk*, *Axin2*, and *Gli1*, the four cSSCs markers independently identified by different groups of investigators (13–16). The cluster analysis indicates that these four cSSCs markers identify cells within the osteogenic cell clusters of all ages, and that these cells significantly diminish as the mice age (Fig. 1 *F–J*). The quantitative analysis (Fig. 1*J*) more specifically shows that in sutures of 4-d-old mice, a significant fraction of the total cells express *Prx1/Prrx1* (~41%) and *Ctsk* (~48%), whereas cells expressing *Gli1* and *Axin 2* are less represented (~10 % and ~8%, respectively). Differently, *Prx1/Prrx1*, *Ctsk*, *Axin2*, and *Gli1* expressing cells are almost absent in the functionally closed sutures of all the older mice (values spanning from ~1 to 2% in 2-mo-old mice to 0.2 to 1% in 14-mo-old mice), confirming that cSSCs significantly diminish in older mice. Collectively, these data indicate that expression of *Prx1/Prrx1*, *Ctsk*, *Gli1*, and *Axin2* markers identifies cells with similar gene expression profiles, suggesting that these cells are all representative of the cSSCs population. Furthermore, the data show a correlation between the elevated number of cSSCs and the actively expanding sutures of 4-d-old mice.

Overlapping Expression of Prx1/Prrx1, Ctsk, Gli1, and Axin2 is Observed in Proliferating cSSCs.
To confirm that expression of *Prx1/Prrx1*, *Ctsk*, *Gli1*, and *Axin2* identifies cells representative of the same cSSCs population, we performed a re-clustering analysis of the osteogenic cells of the sutures of 4-d-old mice. This analysis identified five different subclusters of cells: 1) progenitor cells (PC), 2) proliferative osteogenic cells (PRO), 3) osteoblast precursors (OP), 3) mature osteoblasts (MO), and 4) osteocytes (OC) (Fig. 2*A*) (refer to *Materials and Methods* for the methodology utilized for the classification of the subclusters). Expression of *Prx1/Prrx1*, *Ctsk*, *Gli1*, and *Axin2* significantly overlaps with, and is mainly detectable within, the progenitor cells and, in part, the osteoblast precursors (Fig. 2*B*). A dot plot showing the quantification of the expression of *Prx1/Prrx1* in each of the subclusters confirms that *Prx1/Prrx1* is highly expressed in the progenitor cells subcluster (*SI Appendix*, Fig. S1). Similar trends are observed in the dot plots showing the quantification of the expression of *Axin2*, *Ctsk*, and *Gli1* (*SI Appendix*, Fig. S2). To validate the subclustering analysis and to assess the grade of differentiation of the various subclusters, we performed a pseudotime analysis and visualized the distribution of the subclusters along the obtained trajectory (Fig. 2*C*). This analysis identified the progenitor cell subcluster as the earliest subcluster, while the mature osteoblasts and the osteocytes subclusters are projected at later time points, as the latest subclusters (Fig. 2*C*). When we overlapped the expression of *Prx1/Prrx1* with the pseudotime trajectory, we found *Prx1/Prrx1* to be mainly expressed within the early subclusters (Fig. 2*D*). Similar trends were observed for the expression of *Ctsk*, *Gli1*, and *Axin2* (*SI Appendix*, Fig. S3). A quantitative evaluation of the *Ctsk*, *Gli1*, and *Axin2* expressing cells within the early subclusters (progenitor cells and the proliferative osteogenic cells) shows that the vast majority of these cells (from 92% to 100%) co-express *Prx1/Prrx1* (*SI Appendix*, Table S1). Then, confirming that *Prx1/Prrx1*, *Ctsk*, *Gli1*, and *Axin2* are most
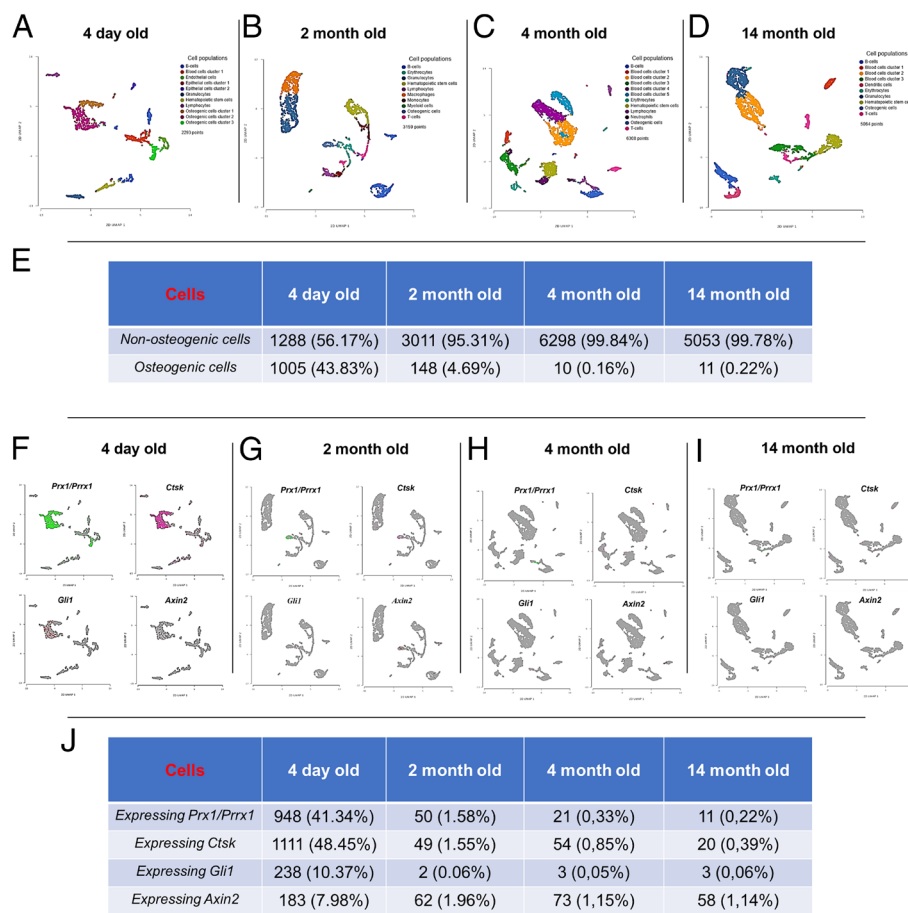
Fig. 1. Single cell RNA-sequencing analysis of 4-d-old, 2-mo-old, 4-mo-old, and 14-mo-old calvarial sutures. (*A–D*) Uniform Manifold Approximation and Projection (UMAP) plot showing unbiased graph-based clusters distribution of all cell populations in sutures isolated from 4-d-old (*A*), 2-mo-old (*B*), 4-mo-old (*C*), and 14-mo-old (*D*) mice. (*E*) Quantification of osteogenic and non-osteogenic cell lineages (absolute numbers counted in each sample and percentages of the total cells within each sample). (*F–I*) UMAPs displaying the expression of Prx1/Prrx1, *Ctsk*, *Gli1*, and *Axin2* in calvarial sutures of 4-d-old (*F*), 2-mo-old (*G*), 4-mo-old (*H*), and 14-mo-old (*I*) mice. (*J*) Quantification of cells expressing *Prx1/Prrx1*, *Ctsk*, *Gli1*, and *Axin2* (absolute numbers counted in each sample and percentages of the total cells within each sample). 4-d-old mice: total cells 2,293 (n = 8); 2-mo-old mice: total cells 3,159 (n = 5); 4-mo-old mice: total cells 6,308 (n = 5); 14-mo-old mice; total cells 5,064 (n = 6).

represented in early differentiation stages of the osteoblastic lineage, we compared their expression to the expression of genes that are associated with more differentiated cells of the osteoblastic lineage. Data show that these genes (*Alpl*, *Runx2*, *Ibsp*, *Sp7*, *Col1a1*, and *Osteocalcin*) are mainly expressed further down into the trajectory (Fig. 2*D*). Since activation of Wnt signaling induces osteoblastic differentiation in cSSCs (13, 28), we further evaluated the level of expression of *β-catenin* and *Tcf7* across the subclusters (*SI Appendix*, Fig. S4). This analysis showed a reduced expression of *β-catenin* and an almost undetectable expression of *Tcf7* in the progenitor cells subcluster, confirming that Wnt signaling is down-regulated in undifferentiated cells of the 4-d-old sutures and up-regulated as cells move into their differentiation path. These data indicate that the expression of *Prx1/Prrx1*, *Ctsk*, *Gli1*, and *Axin2* identifies a population of undifferentiated cells within the sutures of 4-d-old mice. Finally, to assess whether the undifferentiated cells of the sutures are proliferating, we interrogated the scRNA-seq analysis to visualize the expression of *Birc5*, *Ccnd1*, *Espl1*, and *Ki67*, four genes commonly utilized to assess cell proliferation (30–33). This analysis confirms that expression of the proliferation genes is highly detected within *Prx1/Prrx1*, *Axin2*, *Ctsk*, and *Gli1* expressing cells of the 4-d-old sutures (*SI Appendix*, Fig. S5). Collectively, these results indicate that expression of *Prx1/Prrx1*, *Axin2*, *Ctsk*, and *Gli1* identifies undifferentiated and proliferating osteogenic cells within the expanding calvarial sutures of 4-d-old mice.

Expansion of the Sagittal Suture Induces Proliferation of the sSSCs. Since the naturally expanding sutures of the 4-d-old mice are enriched in cSSCs, we next hypothesized that a mechanical expansion of a functionally closed suture of skeletally mature 2-mo-old (8 wk old) mice can reverse engineer what naturally occurs in 4-d-old mice.

More specifically, we hypothesized that the mechanical expansion can induce proliferation of the cSSCs. To test this hypothesis, we utilized 2-mo-old mice, expanded their sagittal suture as previously described (34), and collected the tissue samples after 7 d of expansion (Fig. 3 *A* and *B*). A histological examination confirmed that, after 7 d, the sagittal suture is effectively expanded (Fig. 3*C*). Then, we utilized scRNA-seq to analyze the cellular composition and the gene expression profile of cells of the non-expanded sutures (control, mock surgery) and the expanded sutures (test). As indicated by the UMAPs, the cell cluster analysis identifies a cluster of osteogenic cells in both the expanded and the non-expanded sutures (Fig. 3*D*). However, compared to the osteogenic cells of the non-expanded sutures, the osteogenic cells of the expanded sutures quadruplicate after 7 d of expansion (Fig. 3*E*). On the contrary, after expansion, non-osteogenic cells diminish only by a small percentage (from approximately 99% to 95%) (Fig. 3*E*). More specifically, we found that the cells expressing *Prx1/Prrx1* quadruplicate (from 1.4% to 5.2%), that cells expressing *Ctsk* triplicate (from 2.3% to 6.9%), and that cells expressing *Axin2* or *Gli1* duplicate (from 0.8% to 1.6% and from 0.1% to 0.2%, respectively) (Fig. 3*F*). Then, to test whether the observed cell increase was specific for the cSSCs expressing *Prx1/Prrx1*, *Ctsk*, *Axin 2*, and *Gli1*, we also quantified cells expressing *Runx2*, *Sp7* (*Osterix*), and *Osteocalcin* (*Bglap*), which represent cells more differentiated along the osteoblastic lineage. Data indicate that, contrary to the sSSCs, the more differentiated cells decrease in expanded sutures, with cells expressing Osteocalcin decreasing up to almost 1/3 of the original number (Fig. 3*F*).

An independent experiment, utilizing intravital microscopy (IVM) to quantify *Prx1/Prrx1* expressing cells by means of co-expression of enhanced green fluorescent protein (EGFP) in non-expanded and expanded sagittal sutures of 2-mo-old
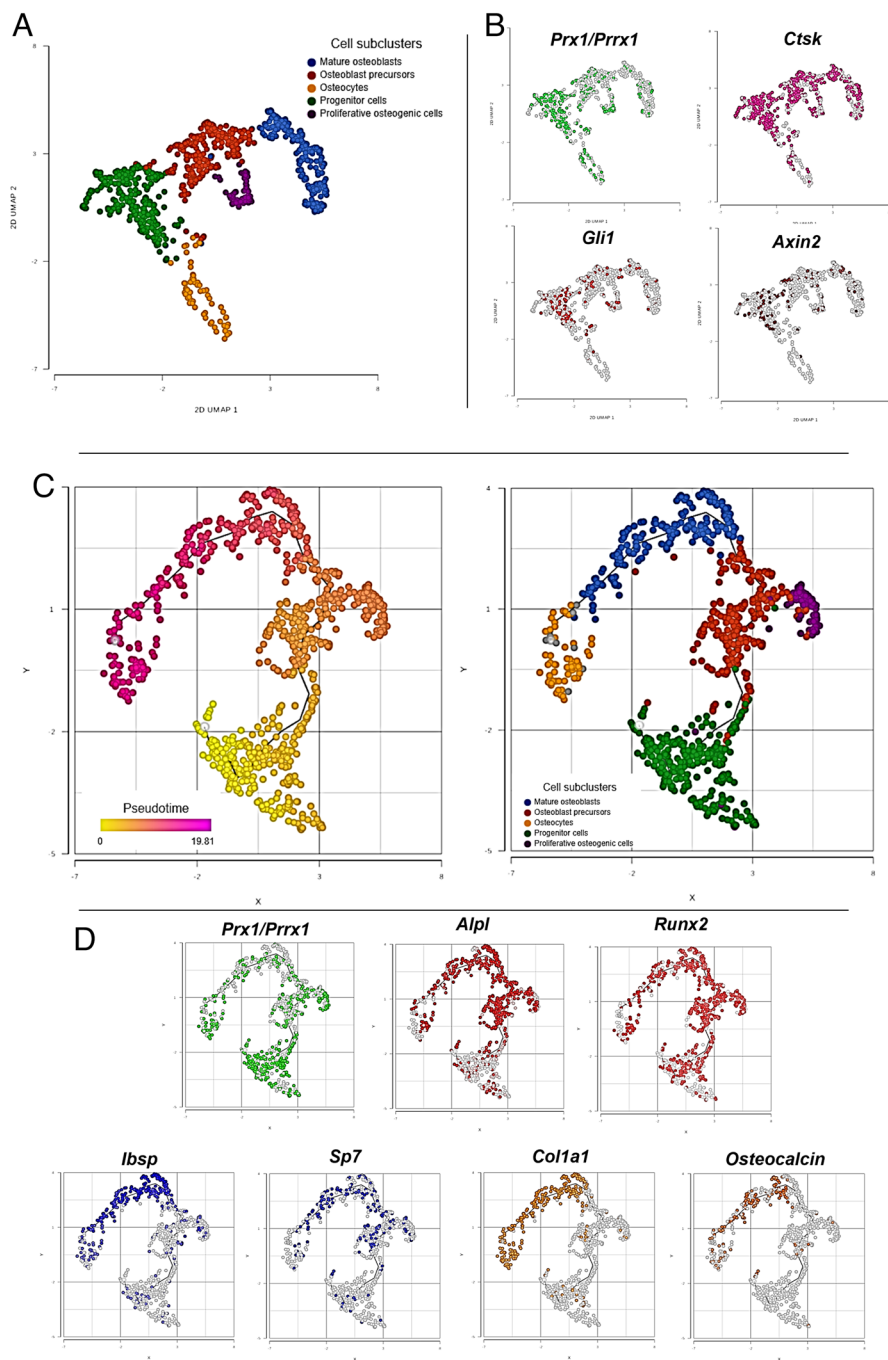
Fig. 2. Subcluster analysis of the osteogenic cells of the expanding sutures of 4-d-old mice. (*A*) UMAP plot showing the identity of the subclusters identified among the osteogenic lineage cells. (*B*) UMAP plots showing the location of cells expressing *Prx1/Prrx1*, *Ctsk*, *Gli1*, and *Axin2*. (*C*) Unbiased trajectory pseudotime analysis of the cells of the osteogenic lineage, from the most undifferentiated (yellow) to the most differentiated (pink). (*D*) Trajectory analysis identifying *Prx1/Prrx1* expressing cells, Alkaline phosphatase (*Alpl*) expressing cells, Bone sialoprotein (*Ibsp*) expressing cells, Osterix (*Sp7*) expressing cells, Collagen type 1(*Col1a1*) expressing cells, and Osteocalcin (*Bglap*) expressing cells.

Prx1-creER-EGFP mice (35), confirms the quantitative scRNA-seq analysis. In fact, when the number of green fluorescent cells were quantified in three different locations along the non-expanded and expanded sagittal sutures of 2-mo-old mice, we found that green fluorescent cells quadruplicate upon expansion (Fig. 3 *G–I*).
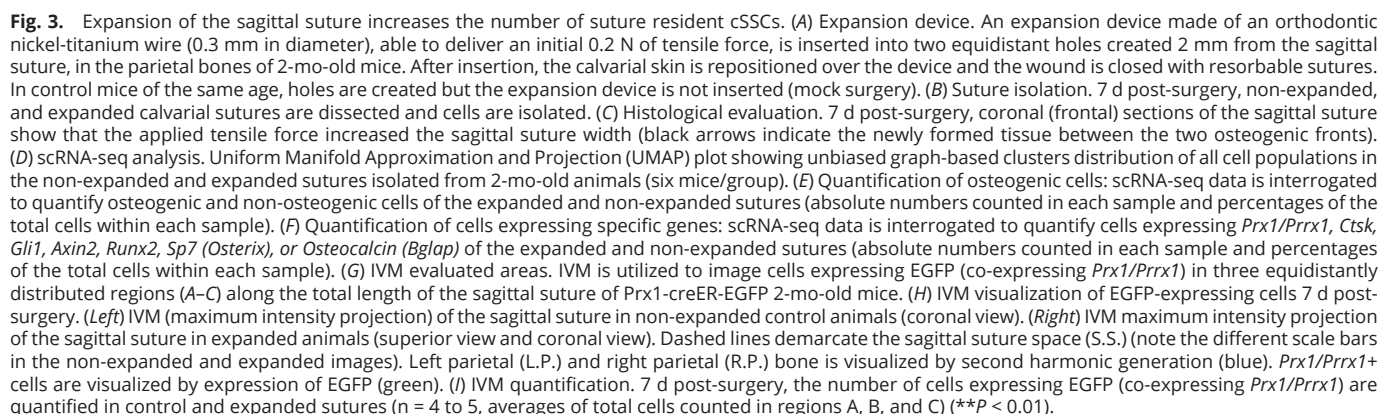
Finally, to test whether the increase of the number of cSSCs during suture expansion is due to proliferation activity, we utilized the scRNA-seq data and quantified the expression of *Birc5*, *Ccnd1*, *Espl1*, and *Ki67* in cells of the expanded and of the non-expanded sutures (Fig. 4). Data indicate that compared to *Prx1/Prrx1* expressing cells of the non-expanded sutures, *Prx1/Prrx1* expressing cells of the expanded sutures present with higher level of expression of all four genes (Fig. 4*A*). Similar results were observed in *Ctsk*, the *Gli1*, and the *Axin2* expressing cells (*SI Appendix,* Fig. S6). On the contrary, more osteoblastic-differentiated cells expressing *Runx2*, *Sp7*, or *Osteocalcin* presented similar levels of

expression of *Birc5*, *Ccnd1*, *Espl1*, and *Ki67* in both non-expanded and expanded sutures (Fig. 4 *B–D*).

An independent evaluation, using quantitative PCR and in situ hybridization, performed 2 d after expansion also confirmed that *Prx1/Prrx1* expressing cells proliferate during the mechanically induced expansion of the sutures (*SI Appendix,* Fig. S7).

Importantly, since Rindone et al (36) recently reported that the creation of a subcritical defect of 1 mm in diameter in the parietal bone can stimulate a significant expansion of the cSSCs, we further analyzed whether the creation of the two 0.25 mm of diameter "anchoring holes" of the expansion device could, per se, induce any significant increase in the number of the cSSCs. To this end, we compared the number of osteogenic and non-osteogenic cells of the 2-mo-old non-surgery mice (as in Fig. 1*E*) with the number of osteogenic and non-osteogenic cells of the 2-mo-old mock surgery mice (no expansion device inserted, as in Fig. 3*E*) and observed no

Fig. 3. Expansion of the sagittal suture increases the number of suture resident cSSCs. (*A*) Expansion device. An expansion device made of an orthodontic nickel-titanium wire (0.3 mm in diameter), able to deliver an initial 0.2 N of tensile force, is inserted into two equidistant holes created 2 mm from the sagittal suture, in the parietal bones of 2-mo-old mice. After insertion, the calvarial skin is repositioned over the device and the wound is closed with resorbable sutures. In control mice of the same age, holes are created but the expansion device is not inserted (mock surgery). (*B*) Suture isolation. 7 d post-surgery, non-expanded, and expanded calvarial sutures are dissected and cells are isolated. (*C*) Histological evaluation. 7 d post-surgery, coronal (frontal) sections of the sagittal suture show that the applied tensile force increased the sagittal suture width (black arrows indicate the newly formed tissue between the two osteogenic fronts). (*D*) scRNA-seq analysis. Uniform Manifold Approximation and Projection (UMAP) plot showing unbiased graph-based clusters distribution of all cell populations in the non-expanded and expanded sutures isolated from 2-mo-old animals (six mice/group). (*E*) Quantification of osteogenic cells: scRNA-seq data is interrogated to quantify osteogenic and non-osteogenic cells of the expanded and non-expanded sutures (absolute numbers counted in each sample and percentages of the total cells within each sample). (*F*) Quantification of cells expressing specific genes: scRNA-seq data is interrogated to quantify cells expressing *Prx1/Prrx1, Ctsk, Gli1, Axin2, Runx2, Sp7 (Osterix)*, or *Osteocalcin (Bglap)* of the expanded and non-expanded sutures (absolute numbers counted in each sample and percentages of the total cells within each sample). (*G*) IVM evaluated areas. IVM is utilized to image cells expressing EGFP (co-expressing *Prx1/Prrx1*) in three equidistantly distributed regions (*A*–*C*) along the total length of the sagittal suture of Prx1-creER-EGFP 2-mo-old mice. (*H*) IVM visualization of EGFP-expressing cells 7 d post-surgery. (*Left*) IVM (maximum intensity projection) of the sagittal suture in non-expanded control animals (coronal view). (*Right*) IVM maximum intensity projection of the sagittal suture in expanded animals (superior view and coronal view). Dashed lines demarcate the sagittal suture space (S.S.) (note the different scale bars in the non-expanded and expanded images). Left parietal (L.P.) and right parietal (R.P.) bone is visualized by second harmonic generation (blue). *Prx1/Prrx1+* cells are visualized by expression of EGFP (green). (*I*) IVM quantification. 7 d post-surgery, the number of cells expressing EGFP (co-expressing *Prx1/Prrx1*) are quantified in control and expanded sutures (n = 4 to 5, averages of total cells counted in regions A, B, and C) (**P < 0.01).

increment in the percentage of the osteogenic cells after the mock surgery. This is also the case for the *Prx1/Prrx1, Ctsk, Gli1*, and *Axin2* expressing cells (compare Fig. 1*J* with Fig. 3*F*). Overall, these data indicate that mechanical expansion of the sagittal sutures increases the number and induces proliferation of the cSSCs

cSSCs of the Mechanically Expanded Sutures and cSSCs of the Naturally Expanding Sutures Present with Similar Gene Expression Profiles. To assess the similarity between the cSSCs of the mechanically expanded sutures of the 2-mo-old mice and the cSSCs of the naturally expanding sutures of the 4-d-old mice, we

Fig. 4. Expansion of the sagittal suture induces expression of *Birc5*, *Ccnd1*, *Espl1*, or *Ki67* in *Prx1/Prrx1* expressing cells. (*A*) scRNA-seq quantification of the expression of *Birc5*, *Ccnd1*, *Espl1*, in *Prx1/Prrx1* expressing cells of non-expanded and expanded sutures. (*B*) scRNA-seq quantification of the expression of *Birc5*, *Ccnd1*, *Espl1*, in *Runx2* expressing cells of non-expanded and expanded sutures. (*C*) scRNA-seq quantification of the expression of *Birc5*, *Ccnd1*, *Espl1*, in *Sp7* expressing cells of non-expanded and expanded sutures. (*D*) scRNA-seq quantification of the expression of *Birc5*, *Ccnd1*, *Espl1*, in *Osteocalcin* expressing cells of non-expanded and expanded sutures. Dots represent single cells and numerical values on the *y* axes indicate the level of expression of the *Birc5*, *Ccnd1*, *Espl1*, or *Ki67* gene. *$P < 0.05$ (six mice/group).

first evaluated the cluster analysis of the mechanically expanded sutures. This analysis shows that, similar to what we observed for the cells of the 4-d-old sutures (Fig. 1), cells expressing *Prx1/Prrx1*, *Ctsk*, *Gi1*, and *Axin2* of the mechanically expanded sutures are almost exclusively located in the osteogenic cells cluster (*SI Appendix,* Fig. S8). Then, we performed a re-clustering analysis of the mechanically expanded osteogenic cells. This analysis identified only two different subclusters of cells: the progenitor cells subcluster

and the osteoblast precursors subcluster (Fig. 5*A*). Expression of *Prx1/Prrx1*, *Ctsk*, *Gli1*, and *Axin2* is detectable in both subclusters (Fig. 5*B*). To assess the grade of differentiation of the two identified subclusters, we performed a pseudotime analysis and visualized the distribution of the subclusters along the obtained trajectory (Fig. 5*C*). Similar to what we found in the naturally expanding sutures of 4-d-old mice, we identified the progenitor cells as the earliest subcluster, while the osteoblast precursors are projected at

later time point (Fig. 5*C*). As expected, when we overlapped the expression of *Prx1/Prrx1* with the pseudotime trajectory, we found *Prx1/Prrx1* to be expressed in both subclusters (Fig. 5*D*), whereas *Ibsp*, *Col1a1*, and *Osteocalcin*, markers of more differentiated osteoblastic cells, are almost undetectable (Fig. 5*D*). Confirming that, in the mechanically expanding sutures, the expression of *Prx1/Prrx1* overlaps with the expression of *Ctsk*, *Gli1*, and *Axin2*, cells, a quantitative evaluation of the cells expressing these genes in the progenitor cells subcluster shows that the vast majority of these cells (from 96% to 100%) co-express *Prx1/Prrx1* (*SI Appendix*, Table S2). A similar result was observed in the naturally expanding sutures (*SI Appendix*, Table S1). Finally, to confirm that the progenitor cells of the mechanically expanding sutures are similar to the progenitor cells of the naturally expanding sutures, we repeated the subclusters

analysis combining the data from both samples (Fig. 6). First, this analysis does not identify any additional subcluster, indicating that there is consistency of clustering between the two samples (Fig. 6*A*). Second, the data indicate that the progenitor cells and the osteoblast precursors of the mechanically expanding sutures overlap with the progenitor cells and the osteoblast precursors of the naturally expanding sutures (Fig. 6*B*). Collectively, these data indicate that cSSCs of the mechanically expanding sutures present with a gene expression profiles that resemble that of the sSSCs of the naturally expanding sutures of 4-d-old animals.

Suture Distraction Enhances Regeneration of Calvarial Critical Size Bone Defects. Since the calvaria of newborn mice is enriched of cSSCs, which resemble, at least in terms of gene expression, the cSSCs of the
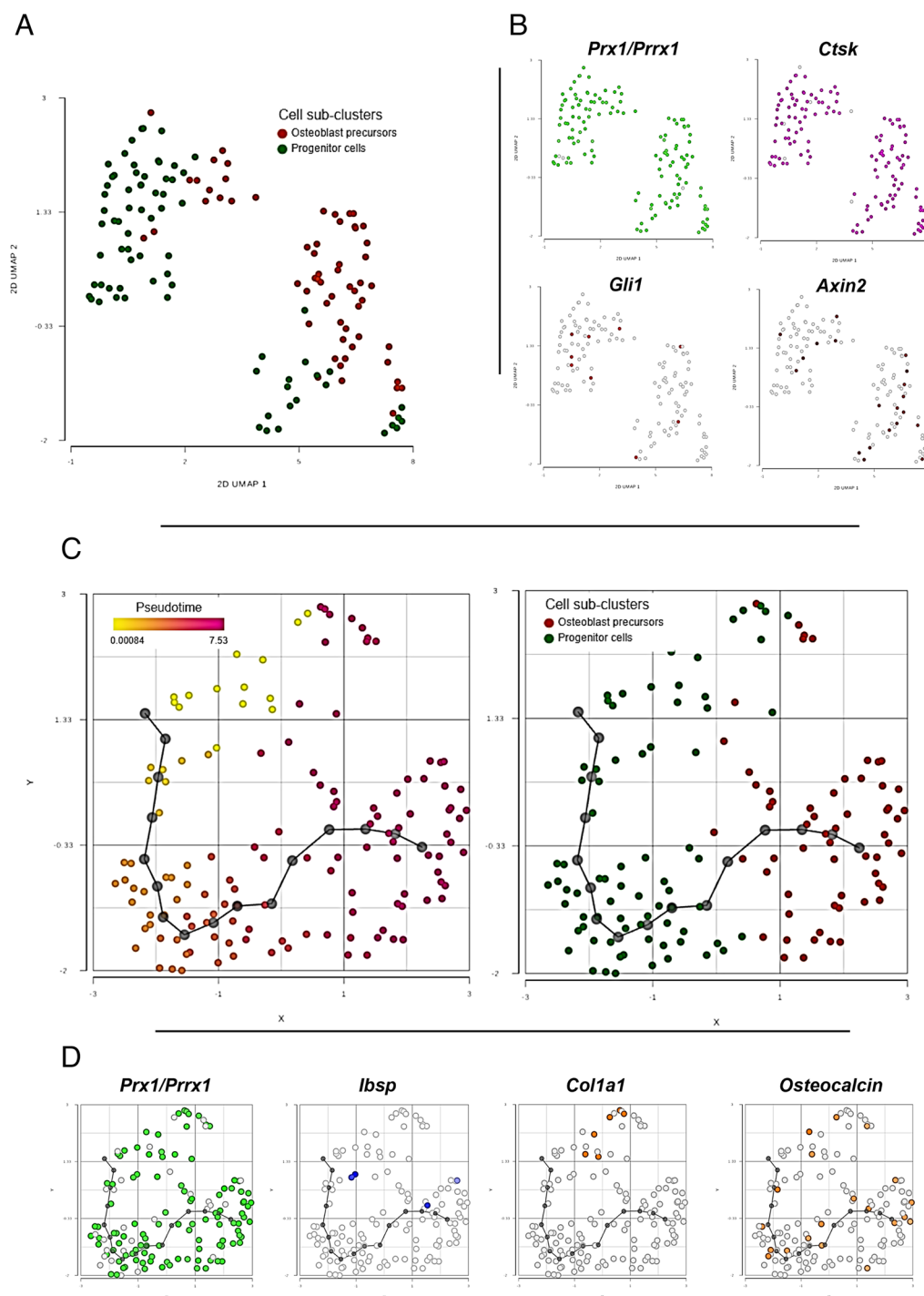
Fig. 5. Subcluster analysis of the osteogenic cells of the mechanically expanded sutures. (*A*) UMAP plot showing the identity of the subclusters identified among the osteogenic lineage cells. (*B*) UMAP plots showing the location of cells expressing *Prx1/Prrx1*, *Ctsk*, *Gli1*, and *Axin2*. (*C*) Unbiased trajectory pseudotime analysis of the cells of the osteogenic lineage, from the most undifferentiated (yellow) to the most differentiated (pink). (*D*) Trajectory analysis identifying *Prx1/Prrx1* expressing cells, *Bone sialoprotein* (*Ibsp*) expressing cells, *Collagen type 1*(*Col1a1*) expressing cells, and *Osteocalcin* (*Bglap*) expressing cells.

mechanically expanded sutures, and since newborn mice can fully regenerate calvarial bone defects, we hypothesized that the mechanical expansion of the functionally closed sagittal suture of 2-mo-old (8 wk old) mice could reverse engineer the spontaneous expanding suture of the newborn mice and could, consequently, sustain the complete regeneration of a c-CSD created in the parietal bone of these skeletally mature mice. To test this hypothesis, simultaneously to the expansion of the sagittal suture, we created a c-CSD within the parietal bone of the mouse calvaria, 3 mm lateral from the sagittal sutures, and 1 mm mesial to the lambdoid suture (*SI Appendix*, Fig. S9). In control mice, the two small holes that would hold the expansion device, as well as a c-CSD, were created in the same locations as in the test mice, but no expansion device was inserted.

Sixty days after surgery, the c-CSDs of the control group showed limited amount of regenerated bone (Fig. 7*A*). On the contrary, the c-CSDs of the test group regenerated up to ~100% of the missing bone (Fig. 7*B*). Microcomputed tomography (μCT) quantification confirmed that the bone volume (BV) and the bone fraction of bone volume over total volume (BV/TV) of the c-CSDs created simultaneously with the suture expansion are significantly higher than the BV and BV/TV of the c-CSDs created in control mice (Fig. 7 *C* and *D*). As expected, since we previously showed that progeny of the cSSCs expressing *Prx1/Prrx1* is responsible for regeneration of calvarila bone defects (13), a lineage tracing analysis performed in Prx1-creER-EGFP;tdTOMATO mice confirmed that the defect in the test mice is regenerated by these cells (*SI Appendix*, Fig. S10).

We conclude that expansion of a functionally closed suture, by means of induced proliferation of the preexisting cSSCs, can sustain regeneration of calvarial bone defect otherwise unable to heal. Importantly, since regeneration does not occur in 10-mo-old mice (*SI Appendix*, Fig. S11), which represents an age in between the 4-mo-old and the 14-mo-old ones analyzed by scRNA-seq, we also propose that the suture expansion-sustained regeneration can occur only when a certain minimum number of preexisting cSSCs are present with the suture.

Wnt Signaling Regulates *Prx1/Prrx1* Expressing Cells of the Expanding Suture during the Regeneration of the Calvarial Critical Size Bone Defects. Since previous studies in our laboratory have shown that *Prx1/Prrx1* expressing

cells are Wnt-responsive cells (13, 28), and since the scRNA-seq analysis of the expanding sutures of 4-d-old mice shows that Wnt signaling is up-regulated in differentiating cells of the osteoblastic lineage (*SI Appendix*, Fig. S4), next we sought to investigate whether Wnt signaling in *Prx1/Prrx1* expressing cells influences the suture expansion-sustained regeneration of the c-CSDs. To this end, we utilized 2-mo-old Prx1-creER-EGFP;β-catenin mice to conditionally inactivate *β-catenin*, and therefore canonical Wnt signaling, by means of cre recombinase (creER) in *Prx1/Prrx1* expressing cells during expansion and during the regeneration process. As indicated by the μCT rendering and by the histological analysis of the defects (Fig. 8 *A* and *B*), we found that the tamoxifen-induced genetic blockade of Wnt signaling in *Prx1/Prrx1* expressing cells significantly impairs the capacity of the c-CSD to regenerate during expansion of the suture. The remodeling of the sagittal suture upon expansion was also impaired by the blockade (Fig. 8*B*). μCT quantification of the regenerated bone in the c-CSDs of *β-catenin* inactivated mice revealed a reduction of the regenerated bone when compared to mice with active canonical Wnt signaling (control), with significant difference in BV and BV/TV (Fig. 8 *C* and *D*). The effective inactivation of Wnt signaling in *Prx1/Prrx1* expressing cells was validated by analyzing the gene expression of *Axin2* (a Wnt target gene) and *β-catenin* in FAC-sorted EGFP+ cells obtained from tamoxifen treated Prx1-creER-EGFP;β-catenin mice (Fig. 8*E*). On the basis of these data, we conclude that canonical Wnt signaling is required during the suture expansion-sustained bone regeneration.

PRX1/PRRX1 Expressing Cells are Located in the Expanding Human Calvarial Sutures. To test the translational significance of the findings observed in the mouse model, we tested whether *PRX1/PRRX1* is expressed in cells of the human sagittal suture. Previous studies in humans have shown that mutation of *PRX1/PRRX1* or deletion of chromosome 1q23.3-q25.1 (the portion of the chromosome 1 that carries the human *PRX1/PRRX1* gene) results in pre- and postnatal growth retardation, with microcephaly, micrognathia, and other skeletal malformations (37–39), thus suggesting that *PRX1/PRRX1* may be expressed in the human calvarial sutures. Confirming that *PRX1/PRRX1* is expressed in the human calvarial sutures, the in situ hybridization in sagittal suture of a human fetus 80 d post-conception shows expression of *PRX1/PRRX1* in cells across the sutures (Fig. 9*A*), giving additional
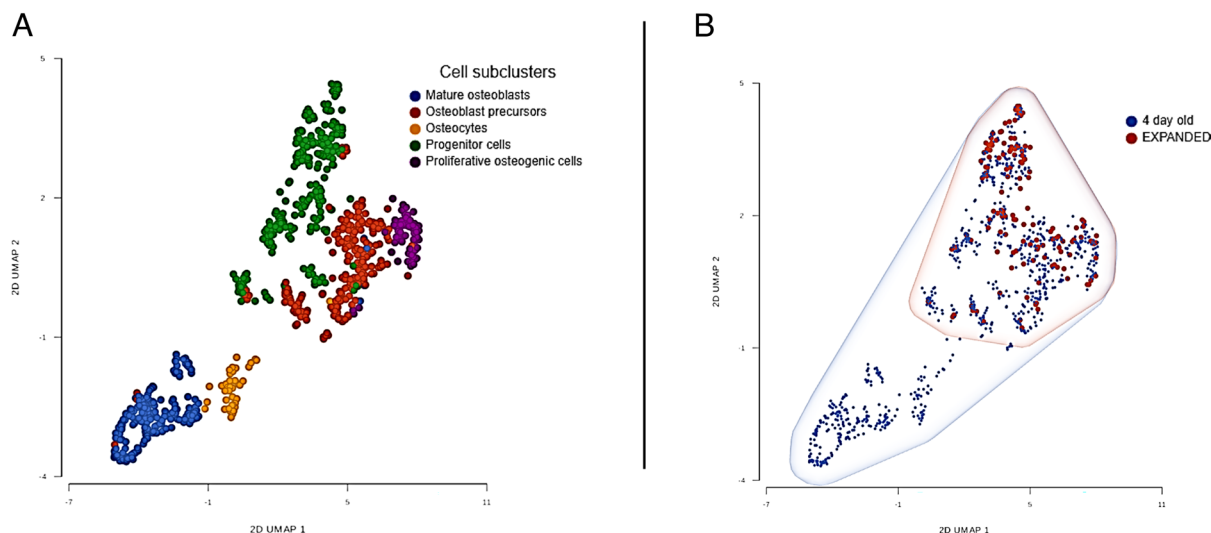
Fig. 6. Subcluster analyses of the osteogenic cells of the mechanically expanded and the naturally expanding sutures. (*A*) UMAP plot showing the identity of the subclusters identified among the osteogenic lineage cells of both samples. (*B*) UMAP plots showing the location of cells of the mechanically expanded sutures (EXPANDED, in red) and of the naturally expanding sutures (4 d old, in blue).
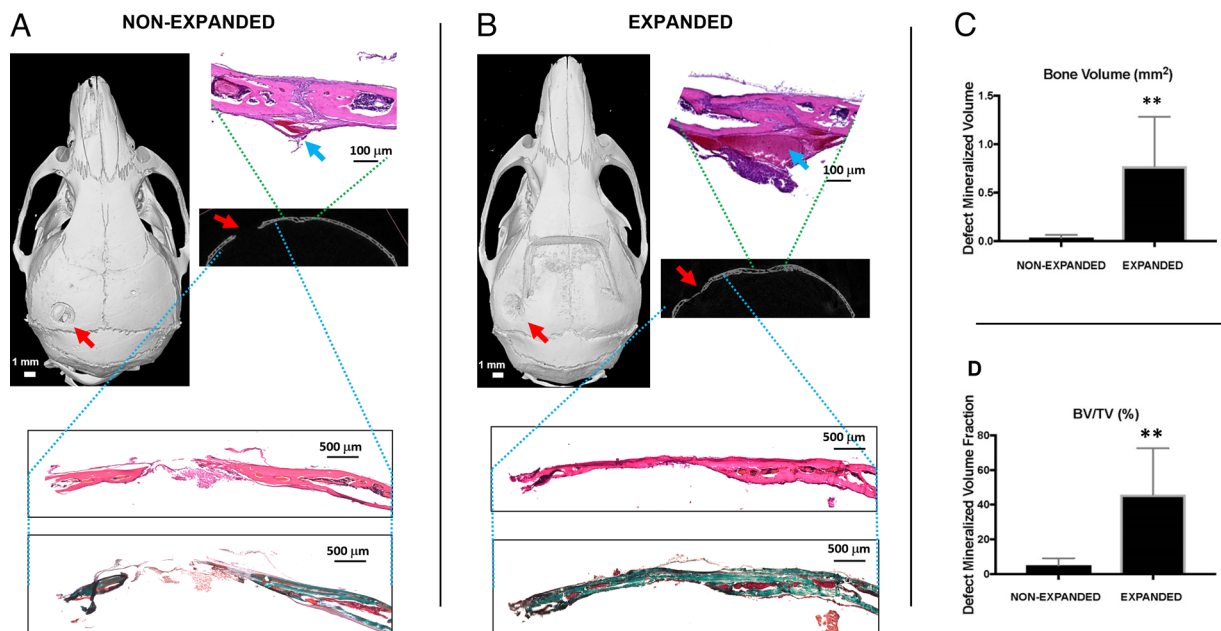
Fig. 7. Expansion of the sagittal suture enhances the regeneration of a c-CSD remotely located from the suture. (*A*) μCT rendering (left, whole skull superior view, with cranial base bones visible through the defect; right, coronal (frontal) section of the parietal bones) and histological sections of the sagittal suture (depicted by green-dashed line) and of the defect (depicted by blue-dashed line) in non-expanded 2-mo-old Prx1-creER-EGFP$^{+/-}$ mice. (*B*) μCT rendering (left, whole skull superior view; right, coronal (frontal) section of the parietal bones) and histological sections of the sagittal suture (depicted by green-dashed line) and of the defect (depicted by blue-dashed line) in expanded 2-mo-old Prx1-creER-EGFP$^{+/-}$ mice. Samples were obtained 60 d after creation of the defects. Red arrows indicate the c-CSD, located 3 mm lateral to the sagittal suture. Blue arrows indicate the sagittal sinus. The implanted radiopaque expansion device can be seen in the coronal view. H&E and Goldner's Trichrome were used for staining unmineralized tissue sections. (*C* and *D*) μCT quantification of bone volume (BV) and of the ratio between bone volume (BV) total volume (TV) regenerated within the c-CSDs, 60 d after surgery (n = 4 to 5, **$P < 0.01$).

evidence of their role in calvarial development. To further confirm that *PRX1/PRRX1* is highly expressed in cells of the human calvarial sutures, we performed a quantitative PCR of the *PRX1/PRRX1* gene in human primary cells obtained from the parietal bone of a human fetus (180 d post-conception) and in human primary cells obtained from the fetal sagittal sutures of six different individuals (at various ages, from 79 d to 108 d post-conception). Results indicate that, compared to the parietal bone cells, sagittal suture cells tend to express higher levels of *PRX1/PRRX1* (in five out of the six tested samples) (Fig. 9*B*). We conclude that *PRX1/PRRX1* is expressed in cells of the human calvaria expanding sutures.
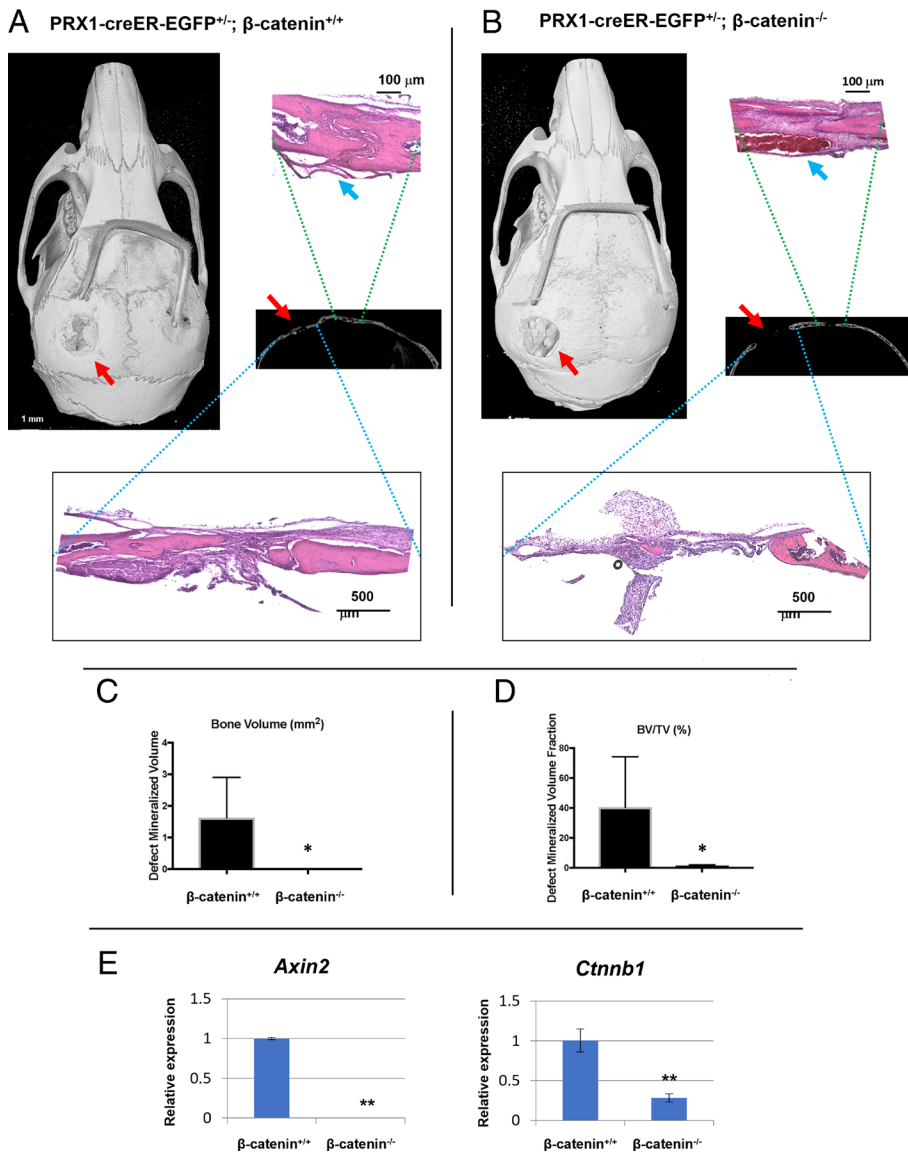
Discussion

Recent studies in the field of craniofacial bone biology have identified the calvarial sutures as reservoirs of skeletal stem cells expressing *Prx1/Prrx1*, or *Ctsk*, *Gli1*, and *Axin2* (13–16). Specifically, we have described the presence of postnatal skeletal stem cells expressing *Prx1/Prrx1* within the calvarial sutures and their requirement for calvarial bone regeneration (13), showing that the regeneration process is abrogated when a significant number of *Prx1/Prrx1* expressing cells are ablated by means of a targeted expression of Diphtheria toxin. Transplanting sutures carrying traceable fluorescent *Prx1/Prrx1* expressing cells, we also showed that the calvarial bone regeneration occurs by means of their progeny. Building upon these studies, now we show for the first time that there is a significant overlap of expression of *Prx1/Prrx1* in *Ctsk*, *Gli1*, and *Axin2* expressing cells, indicating that expression of *Prx1/Prrx1*, *Axin2*, *Ctsk*, and *Gli1* identifies the cSSCs population of the calvarial sutures.

While most of the current approaches to bone regenerative therapies focus on transplantation of bone competent cells, or on implantation of osteoconductive or osteoinductive biomaterials (40), here we posited that such approaches, which are not exempt of health risks, may not be necessary if the regenerative potential of the native

cSSCs is fully exploited. Since in children up to 2 y of age, with expanding osteogenically active calvarial sutures, regeneration of calvarial bone defects occurs naturally and without therapeutic aids, (17, 18), we hypothesized that the expanding sutures, with their high content of cSSCs, are responsible for this extraordinary regeneration potential. Therefore, using the skeletally mature 2-mo-old (8 wk old) mouse calvaria as a model, we aimed at demonstrating that if an otherwise functionally closed suture is artificially expanded, its content of cSSCs increases, and complete regeneration of a bone defect, even critical in size and remotely located from the suture, can occur. A scRNA-seq analysis of the cells of the calvarial sutures, performed in mice of different ages, from 4-d-old up to 14-mo-old mice, demonstrated that the naturally expanding sutures of the 4-d-old mice are highly enriched with cSSCs. Subsequently, we demonstrated that a tensile force applied to a mature functionally closed suture can induce an enrichment in the number of the cSSCs and can sustain the regeneration of calvarial bone defects otherwise unable to regenerate. Therefore, the artificial expansion of a functionally closed, skeletally mature, suture can be utilized to harness the cSSCs and foster regeneration of calvarial bone defects. Importantly, our studies also show that the suture expansion strategy has limitations, since it is not effective in 10-mo-old mice, when the number of resident cSSCs is expected to be limited. This limitation is probably due to the cSSCs present in the 10-mo-old sutures, which may be either too limited in number or senescent to be able to proliferate up to a sufficiently higher number able to sustain the regeneration process. Thus, the suture expansion-sustained regeneration strategy has a limited temporal window of efficacy, although still effective in skeletally mature 2-mo-old mice.

Of interest in the present studies is the fact that the regeneration of a c-CSD occurs even when the c-CSD is positioned at a considerable distance from the suture. In fact, Park et al. (26) have shown that the healing capacity of a c-CSD in the mouse calvaria decreases with increasing distance from the sutures, as c-CSD distant 1 mm

A PRX1-creER-EGFP$^{+/-}$; β-catenin$^{+/+}$

B PRX1-creER-EGFP$^{+/-}$; β-catenin$^{-/-}$

C Bone Volume (mm^2)

D BV/TV (%)

E *Axin2*   *Ctnnb1*

Fig. 8. Regeneration of c-CSDs sustained by mechanical expansion of the sagittal suture is mediated by Wnt signaling. (*A*) µCT rendering (whole skull superior view and coronal (frontal) section of the parietal bones) and histological sections of the sagittal suture (depicted by green-dashed line) and of the c-CSD (depicted by blue-dashed line) in suture expanded 2-mo-old Prx1-creER-EGFP$^{+/-}$; β-catenin$^{+/+}$ mice 60 d after creation of the defect. (*B*) µCT rendering (whole skull superior view with cranial base bones visible through the defect, and coronal (frontal) section of the parietal bones) and histological sections of the sagittal suture (depicted by green-dashed line) and of the c-CSD (depicted by blue-dashed line) in suture expanded 8-wk-old Prx1-creER-EGFP$^{+/-}$; β-catenin$^{-/-}$ mice 60 d after creation of the defect. Red arrows indicate the c-CSD, located 3 mm lateral to the sagittal suture. Blue arrows indicate the sagittal sinus. (*C*) µCT quantification of the regenerated bone volume (BV) in c-CSDs 60 d after surgery (n = 5). (*D*) µCT quantification of regenerated bone volume (BV)/total volume (TV) in c-CSDs 60 d after surgery (n = 5). (*E*) qPCR of canonical Wnt signaling responsive genes (*Axin2* and *β-catenin* (*Ctnnb1*)) in Prx1/Prrx1 expressing cells isolated from Prx1-creER-EGFP$^{+/-}$; β-catenin$^{+/+}$ and Prx1-creER-EGFP$^{+/-}$; β-catenin$^{-/-}$ mice treated with tamoxifen (six pooled mice/group, two technical replicates/group). All mice were treated with tamoxifen for 10 d, starting 5 d before surgery. *$P < 0.05$, **$P < 0.01$.

from the sagittal suture is able to regenerate ~50% of the missing bone while a c-CSDs distant 2 mm from the suture is able to regenerate only ~20% of the missing bone (26). Thus, the suture expansion-sustained regeneration of a defect positioned 3 mm from the sagittal expanding sutures and 1 mm from the lambdoid suture is quite remarkable. The regeneration of remotely located defects also distinguishes the suture expansion-sustained regeneration from the traditional distraction osteogenesis, whereby bone formation is limited within the distraction site. While similar molecular mechanisms may regulate the osteogenic activity within the tension sites of the expanded sutures and the distracted bone segments, the ability of the cSSCs, or their progeny, to reach a distant defect during suture expansion is regulated by cellular migrating mechanisms not necessarily activated during distraction osteogenesis. Regardless of the mechanisms responsible for the cell migration and the remote regeneration process, the current study demonstrates that they depend on the activation of Wnt signaling within the *Prx1/Prrx1* expressing cell during the regeneration process. This conclusion is validated by existing studies showing that Wnt signaling is involved with craniofacial development (41), as well as calvarial suture homeostasis (41, 42, 28) and calvarial bone regeneration (43), and that is activated by tension forces applied to teeth during orthodontic treatments (44) and required for distraction osteogenesis of long bones (45).

With the goal of investigating the translational significance of the mouse studies, we investigated whether expression of *PRX1/PRRX1* could also be detected in cells of the human calvarial sutures. We found that, similar to cells of the mouse sutures, cells of the human fetal sutures (in situ hybridization) and primary cells derived from the fetal sutures (in vitro qPCR assays) express PRX1/PRRX1. This result, along with the documented involvement of mutations of the *PRX1/PRRX1* gene with craniofacial malformations (37, 38, 46), proves that *PRX1/PRRX1* expressing cells have a significant role in the craniofacial development and might, consequently, have a role in the regeneration of the human calvarial bone defects as well. We propose that the translational meaning of the present studies is quite significant since we showed that, at least in mice, the suture expansion-sustained bone regeneration process does not require transplantation of osteogenic tissue or implantation of any biomaterial or scaffold within the bone defects. Since bone distraction devices are commonly utilized in humans to correct craniosynostosis and other craniofacial malformation (47, 48), and since resorbable devices have been recently developed to eliminate the need for a second operative procedure for hardware removal (49), clinical studies could be performed to test this bone regeneration approach. Importantly, given the age-associated limitations that we observed in mice,
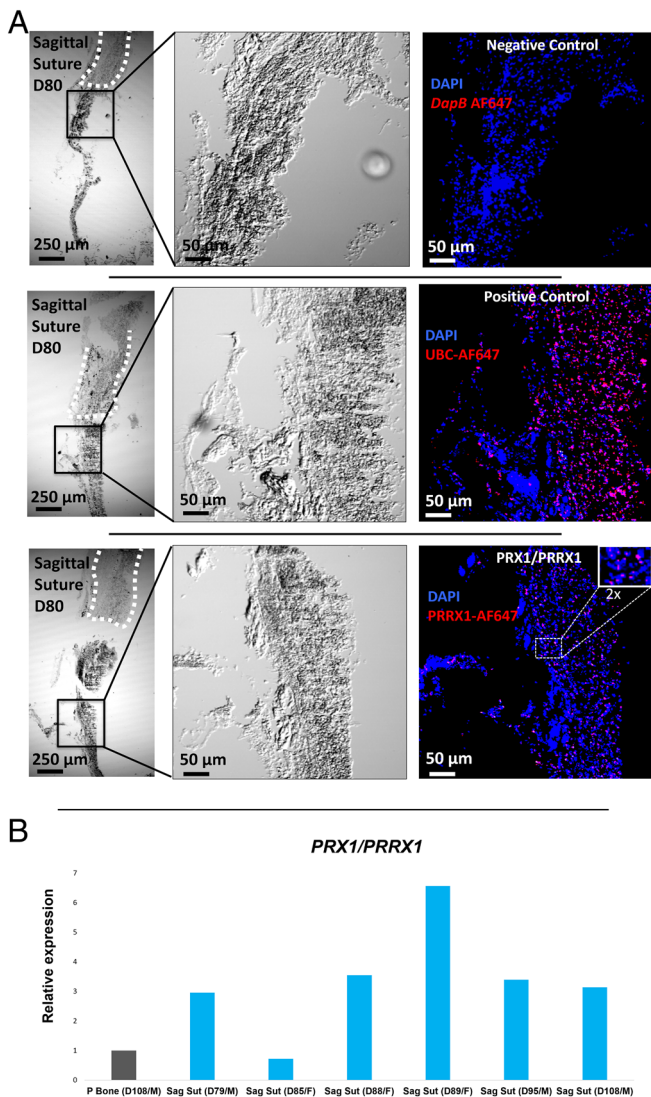
Fig. 9. *PRX1/PRRX1* is expressed in human calvarial sutures. (*A*) In situ hybridization in the sagittal suture of human fetal calvaria (Day 80 post-conception). (*Top*) Negative control targeting *DapB* bacterial gene (DapB-AF647) demonstrates no detectable signal. (*Middle*) Positive control targeting *POLYUBIQUITIN-C* (UBC-AF647) is detected in most of the cells. (*Bottom*) Sections stained with the probe targeting human *PRX1/PRRX1* (PRRX1-AF647) present with signal in a discrete number of suture cells (see 2× *Inset*). Dashed lines (*Left*) identify calvarial bones. (*B*) Quantitative RT-PCR analysis of gene expression in primary cells isolated from the parietal bone and from the sagittal suture of human fetal calvaria. Quantitative PCR was performed to assess the expression of *PRX1/PRRX1* in primary cells derived from the parietal bone (P Bone) and from the sagittal suture (Sag Sut). Post-conception age and sex of the fetus are shown in parentheses.

future clinical studies should assess these limitations in humans as well. Thus, calvarial sutures could represent targetable auto-therapy entities whose local stimulation may sustain regeneration of otherwise non-healing calvarial bone defects.

Finally, expanding on the calvarial clinical application, since *Prx1/Prrx1* expressing cells are present within the periosteum of long bones and significantly contribute to the healing of long bone fractures (50, 51), one may translate the results of the present calvarial studies to the regeneration of defects in long bones. For instance, special minimally invasive devices could be engineered to deliver a tensile tenting force to the periosteum of the long bones to induce activation of the periosteum and sustain the regeneration of otherwise non-healing fractures, even when they are remotely located (i.e., expansion of the diaphyseal periosteum for healing of the femur's head fractures).

In conclusion, our studies may lead to the development of more effective bone regenerating autotherapies for humans, whereby the endogenous healing capacity of each patient is fully exploited by stimulating the stem cell niches, such as the calvarial sutures, to harness their content of SSCs and sustain bone regeneration, even in remotely located sites.

Methods

A summary of the Methods is reported below. Please refer to *SI Appendix* for additional details.

Animals. Experiments were conducted in compliance with the Guide for the Care and Use of Laboratory Animals at the University of Pittsburgh School of Dental Medicine (IACUC Protocol #: 20066890) and at the Harvard School of Dental School (IACUC Protocol # IS00000535). To optimize the quantification of the fluorochrome expression and minimize signal noise observed in female mice (13), only Prx1-creER-EGFP male mice were utilized for the IVM quantification studies. Accordingly, only male mice (C57BL/6) were also utilized for the scRNA-seq studies. Male and female mice (C57BL/6 and Prx1-creER-EGFP;β-catenin) were randomly distributed in each group for the bone regeneration studies.

Single Cell RNA Sequencing. Cells were isolated using collagenase digestions, and scRNA-seq was performed using Chromium Next GEM Single Cell 3′ GEM, Library & Gel Bead Kit v3.1 (10× Genomics, USA) following the manufacturer's guidelines. The subsequent data analysis, including statistical evaluations, was performed using *Partek® Flow®* software, v10.0 (Partek, Inc.). Clusters and subcluster were identified first by using an unbiased bioinformatic approach, in which we attributed cell identities using the Partek® *Flow®* software's "Biomarker" function, obtaining a list of the top 25 most expressed genes by each cluster or subcluster (*SI Appendix*, Tables S3–S10). Second, we compared the expression of the cell identifiers obtained by Partek® with preexisting and published data (52, 53).

Mouse Suture Expansion Surgery and Creation of Calvarial Bone Defects. Mice were anesthetized, a surgical incision was performed to expose the calvarial bones, and the expansion device was applied. Then, the incision was closed to fully cover the expansion device (*SI Appendix*, Fig. S9). Control mock surgery (non-expanded group) replicated every step of the surgical procedure, but expansion device was not inserted.

For the bone regeneration studies, immediately after insertion of the suture expander, a defect of a diameter of 2.0 mm was manually created in the left parietal bone.

In Vivo Imaging and Quantification of Mouse *Prx1/Prrx1* expressing Cells. Intravital microscopy and Prx1-creER-EGFP^{+/−} transgenic male mice were utilized for in vivo imaging and in vivo quantification of green fluorescent *Prx1/Prrx1* expressing cells according to a methodology previously described (13, 27).

In Situ Hybridization in Mouse Sagittal Sutures. To perform in situ hybridization, the RNAscope Multiplex Fluorescent Reagent Kit V2 (320850, RNAscope®, Advanced Cell Diagnostics, Inc., Newark, CA) was used according to manufacturer's recommendations.

qPCR of Mouse *Prx1/Prrx1* expressing Cells. EGFP+ cells, co-expressing *Prx1/Prrx1*, were sorted (average of 100 to 150 cells/animal), and gene expression analyses were performed using the single cell to CT kit (Thermo Fisher Scientific, City and State).

Micro-CT Analyses of Mouse Cranium. Mouse skulls were scanned using a Scanco µCT40 scanner (Scanco Medical AG, Basserdorf, Switzerland). Bone segmentation was conducted at a threshold of 300 (scale: 0 to 1,000), and the volume of interest (VOI) investigated included the 2 mm segmental defect and additional 0.5 mm in the peripheral regions.

Inducible Inactivation of Canonical Wnt Signaling in Mouse *Prx1/Prrx1* expressing Cells. Prx1-creER-EGFP^{+/−}; β-catenin^{+/+} mice and Prx1-creER-EGFP^{+/−}; β-catenin^{fl/fl} mice (identified in the figures as Prx1-creER-EGFP^{+/−}; β-catenin^{−/−} mice to indicate the cre recombinase inactivation of the β-catenin gene) were injected with tamoxifen (intraperitoneally, 40 mg/Kg in sterile corn oil) 5 d before and 5 d after surgery.

In Situ Hybridization of Human Sagittal Sutures. De-identified specimen of the human fetal calvarial tissue (age 80 d post-conception) was obtained from the Birth Defects Research Laboratory at the University of Washington. The RNAscope Multiplex Fluorescent Reagent Kit V2 (320850, RNAscope®, Advanced Cell Diagnostics, Inc., Newark, CA) was used according to manufacturer's recommendations.

qPCR of Human Sagittal Suture Cells. De-identified specimens from human fetal calvarial tissue (age 79 to 108 d post-conception) were obtained from the Birth Defects Research Laboratory at the University of Washington. Immediately after collection, the parietal bone tissue or the sagittal suture tissue was dissected and cells were isolated as previously described (54). After culturing, cells were dissociated from respective plates, and RNA was immediately isolated with the High Pure miRNA Isolation Kit (Roche, Basel, Switzerland) per manufacturer instructions. qPCR reactions were carried out using the TaqMan gene expression analysis kit.

Statistical analyses of μCT and qPCR data. Student's t test was utilized to identify statistically significant difference among the analyzed groups of mice or genes.

Data, Materials, and Software Availability. All study data are included in the article and/or SI Appendix. The scRNA-seq data discussed in this publication have been deposited in NCBI's Gene Expression Omnibus (Edgar et al., 2002) and are accessible through GEO Series accession number GSE227468 (https://www.ncbi.nlm.nih.gov/geo/query/acc.cgi?acc=GSE227468).

Author affiliations: [a]Department of Oral Medicine, Infection, and Immunity, Harvard School of Dental Medicine, Boston, MA 02115; [b]Department of Biomedical Dental Sciences, College of Dentistry, Imam Abdulrahman Bin Faisal University, Dammam 34212, Saudi Arabia; [c]Department of Periodontics and Preventive Dentistry, University of Pittsburgh School of Dental Medicine, Pittsburgh, PA 15261; [d]Center for Craniofacial Regeneration, University of Pittsburgh School of Dental Medicine, Pittsburgh, PA 15261; [e]Advanced Microscopy Program, Center for Systems Biology and Wellman Center for Photomedicine, Massachusetts General Hospital, Boston, MA 02114; [f]Center for Developmental Biology and Regenerative Medicine, Seattle Children's Research Institute, Seattle, WA 98101; [g]Division of Craniofacial Medicine, Department of Pediatrics, University of Washington, Seattle, WA 98195; [h]Department of Medicine, University of Pittsburgh School of Medicine, Pittsburgh, PA 15261; [i]University of Pittsburgh UPMC Hillman Cancer Center, Pittsburgh, PA 15232; and [j]McGowan Institute for Regenerative Medicine, University of Pittsburgh, Pittsburgh, PA 15219

1. J. A. Fearon, D. Griner, K. Ditthakasem, M. Herbert, Autogenous bone reconstruction of large secondary skull defects. *Plast Reconstr Surg.* **139**, 427–438 (2017).
2. A. Abu-Ghname et al., Outcomes and complications of pediatric cranioplasty: A systematic review. *Plast. Reconstr. Surg.* **144**, 433e–443e (2019).
3. S. E. C. M. van de Vijfeijken et al., Factors related to failure of autologous cranial reconstructions after decompressive craniectomy. *J. Craniomaxillofac. Surg.* **47**, 1420-1425 (2019).
4. M. Czerwinski, R. A. Hopper, J. Gruss, J. A. Fearon, Major morbidity and mortality rates in craniofacial surgery: An analysis of 8101 major procedures. *Plast Reconstr. Surg.* **126**, 181–186 (2010).
5. R. Tevlin et al., Biomaterials for craniofacial bone engineering. *J. Dent Res.* **93**, 1187–1195 (2014).
6. E. J. Woo, Adverse events reported after the use of recombinant human bone morphogenetic protein 2. *J. Oral Maxillofac. Surg.* **70**, 765–777 (2012).
7. A. Mesfin et al., High-dose rhBMP-2 for adults: Major and minor complications: A study of 502 spine cases. *J. Bone Joint Surg. Am.* **95**, 1546–1553 (2013).
8. P. A. Zuk, Tissue engineering craniofacial defects with adult stem cells? Are we ready yet? *Pediatr. Res.* **63**, 478–486 (2008).
9. K. G. Marra, J. P. Rubin, The potential of adipose-derived stem cells in craniofacial repair and regeneration. *Birth Defects Res. C Embryo Today* **96**, 95–97 (2012).
10. D. H. Doro, A. E. Grigoriadis, K. J. Liu, Calvarial suture-derived stem cells and their contribution to cranial bone repair. *Front. Physiol.* **8**, 956 (2017).
11. J. F. Martin, E. N. Olson, Identification of a prx1 limb enhancer. *Genesis* **26**, 225–229 (2000).
12. M. Logan et al., Expression of Cre recombinase in the developing mouse limb bud driven by a Prxl enhancer. *Genesis* **33**, 77–80 (2002).
13. K. Wilk et al., Postnatal calvarial skeletal stem cells expressing PRX1 reside exclusively in the calvarial sutures and are required for bone regeneration. *Stem Cell Rep.* **8**, 933–946 (2017).
14. H. Zhao et al., The suture provides a niche for mesenchymal stem cells of craniofacial bones. *Nat. Cell Biol.* **17**, 386–396 (2015).
15. T. Maruyama, J. Jeong, T.-J. Sheu, W. Hsu, Stem cells of the suture mesenchyme in craniofacial bone development, repair and regeneration. *Nat. Commun.* **7**, 10526 (2016).
16. S. Debnath et al., Discovery of a periosteal stem cell mediating intramembranous bone formation. *Nature* **562**, 133–139 (2018).
17. O. O. Aalami et al., Applications of a mouse model of calvarial healing: Differences in regenerative abilities of juveniles and adults. *Plast Reconstr. Surg.* **114**, 713–720 (2004).
18. K. Sirola, Regeneration of defects in the calvaria. An experimental study. *Ann. Med. Exp. Biol. Fenn.* **38**, 1–87 (1960).
19. J. J. Pritchard, J. H. Scott, F. G. Girgis, The structure and development of cranial and facial sutures. *J. Anat.* **90**, 73–86 (1956).
20. G. M. Morriss-Kay, A. O. M. Wilkie, Growth of the normal skull vault and its alteration in craniosynostosis: Insights from human genetics and experimental studies. *J. Anat.* **207**, 637–653 (2005).
21. M. Grova et al., Models of cranial suture biology. *J. Craniofac Surg.* **23**, 1954–1958 (2012).
22. M. A. Ignelzi, Y. H. Liu, R. E. Maxson, M. L. Snead, Genetically engineered mice: Tools to understand craniofacial development. *Crit. Rev. Oral Biol. Med.* **6**, 181–201 (1995).
23. G. Holmes, The role of vertebrate models in understanding craniosynostosis. *Childs Nerv. Syst.* **28**, 1471–1481 (2012).
24. S. Menon et al., Skeletal stem and progenitor cells maintain cranial suture patency and prevent craniosynostosis. *Nat. Commun.* **12**, 4640 (2021).
25. M. P. Murphy, N. Quarto, M. T. Longaker, D. C. Wan, * Calvarial defects: Cell-based reconstructive strategies in the murine model. *Tissue Eng. C Methods.* **23**, 971–981 (2017).
26. S. Park, H. Zhao, M. Urata, Y. Chai, Sutures possess strong regenerative capacity for calvarial bone injury. *Stem Cells Dev.* **25**, 1801–1807 (2016).
27. C. Lo Celso et al., Live-animal tracking of individual haematopoietic stem/progenitor cells in their niche. *Nature* **457**, 92–96 (2009).
28. S.-C.A. Yeh, K. Wilk, C. P. Lin, G. Intini, In vivo 3D histomorphometry quantifies bone apposition and skeletal progenitor cell differentiation. *Sci. Rep.* **8**, 5580 (2018).
29. A. Marghoub et al., Characterizing and modeling bone formation during mouse calvarial development. *Phys. Rev. Lett.* **122**, 048103 (2019).
30. T. Scholzen, J. Gerdes, The Ki-67 protein: From the known and the unknown. *J. Cell Physiol.* **182**, 311–322 (2000).
31. I. Matsuura et al., Cyclin-dependent kinases regulate the antiproliferative function of Smads. *Nature* **430**, 226–231 (2004).
32. S. Hauf, I. C. Waizenegger, J. M. Peters, Cohesin cleavage by separase required for anaphase and cytokinesis in human cells. *Science* **293**, 1320–1323 (2001).
33. F. Li et al., Control of apoptosis and mitotic spindle checkpoint by survivin. *Nature* **396**, 580–584 (1998).
34. N. Takeshita et al., In vivo expression and regulation of genes associated with vascularization during early response of sutures to tensile force. *J. Bone Miner. Metab.* **35**, 40–51 (2017).
35. A. Kawanami, T. Matsushita, Y. Y. Chan, S. Murakami, Mice expressing GFP and CreER in osteochondro progenitor cells in the periosteum. *Biochem. Biophys. Res. Commun.* **386**, 477–482 (2009).
36. A. N. Rindone et al., Quantitative 3D imaging of the cranial microvascular environment at single-cell resolution. *Nat. Commun.* **12**, 6219 (2021).
37. F. Lam, C. Morris, Nine year old boy with chromosome 1q23.3-q25.1 deletion. *Am. J. Med. Genet A.* **170**, 3013–3017 (2016).
38. C. Sergi, D. Kamnasaran, PRRX1 is mutated in a fetus with agnathia-otocephaly. *Clin. Genet.* **79**, 293–295 (2011).
39. A. T. Timberlake et al., De novo mutations in the BMP signaling pathway in lambdoid craniosynostosis. *Hum. Genet.* **142**, 21–32 (2023).
40. M. R. Borrelli, M. S. Hu, M. T. Longaker, H. P. Lorenz, Tissue engineering and regenerative medicine in craniofacial reconstruction and facial aesthetics. *J. Craniofac Surg.* **31**, 15–27 (2020).
41. P. Mani, A. Jarrell, J. Myers, R. Atit, Visualizing canonical Wnt signaling during mouse craniofacial development. *Dev. Dyn.* **239**, 354–363 (2010).
42. Y. Mishina, T. N. Snider, Neural crest cell signaling pathways critical to cranial bone development and pathology. *Exp. Cell Res.* **325**, 138–147 (2014).
43. S. Minear et al., Wnt proteins promote bone regeneration. *Sci. Transl. Med.* **2**, 29ra30 (2010).
44. H.-D. Fu, B.-K. Wang, Z.-Q. Wan, H. Lin, M.-L. Chang et al., Wnt5a mediated canonical Wnt signaling pathway activation in orthodontic tooth movement. *J. Mol. Histol.* **47**, 455–466 (2016).
45. X. Wang et al., Wnt/β-catenin signaling is required for distraction osteogenesis in rats. *Connect. Tissue Res.* **59**, 45–54 (2018).
46. M. Donnelly, E. Todd, M. Wheeler, V. D. Winn, D. Kamnasaran, Prenatal diagnosis and identification of heterozygous frameshift mutation in PRRX1 in an infant with agnathia-otocephaly. *Prenat. Diagn.* **32**, 903–905 (2012).
47. R. Winters, S. A. Tatum, Craniofacial distraction osteogenesis. *Facial Plast. Surg. Clin. North Am.* **22**, 653–664 (2014).
48. J. G. McCarthy et al., Parameters of care for craniosynostosis. *Cleft Palate Craniofac. J.* **49**, 1S–24S (2012).
49. F. D. Burstein et al., Single-stage craniofacial distraction using resorbable devices. *J. Craniofac. Surg.* **13**, 776–782 (2002).
50. O. Duchamp de Lageneste et al., Periosteum contains skeletal stem cells with high bone regenerative potential controlled by Periostin. *Nat. Commun.* **9**, 773 (2018).
51. A. Esposito, L. Wang, T. Li, M. Miranda, A. Spagnoli, Role of Prx1-expressing skeletal cells and Prx1-expression in fracture repair. *Bone* **139**, 115521 (2020).
52. G. Holmes et al., Integrated transcriptome and network analysis reveals spatiotemporal dynamics of calvarial suturogenesis. *Cell Rep.* **32**, 107871 (2020).
53. D. T. Farmer et al., The developing mouse coronal suture at single-cell resolution. *Nat. Commun.* **12**, 4797 (2021).
54. N. Homayounfar et al., Transcriptional analysis of human cranial compartments with different embryonic origins. *Arch. Oral. Biol.* **60**, 1450–1460 (2015).